

ROM2F/2008/02
submitted for publication

Investigation on light dark matter

R. Bernabei^{a,b}, P. Belli^b, F. Cappella^{c,d}, R. Cerulli^e, C.J. Dai^f, H.L. He^f,
A. Incicchitti^d, H.H. Kuang^f, J.M. Ma^f, X.H. Ma^f, F. Montecchia^{a,b},
F. Nozzoli^{a,b}, D. Prospero^{c,d}, X.D. Sheng^f, Z.P. Ye^{f,g}, R.G. Wang^f,
Y.J. Zhang^f

^a*Dip. di Fisica, Università di Roma “Tor Vergata”, I-00133 Rome, Italy*

^b*INFN, sez. Roma “Tor Vergata”, I-00133 Rome, Italy*

^c*Dip. di Fisica, Università di Roma “La Sapienza”, I-00185 Rome, Italy*

^d*INFN, sez. Roma, I-00185 Rome, Italy*

^e*Laboratori Nazionali del Gran Sasso, I.N.F.N., Assergi, Italy*

^f*IHEP, Chinese Academy, P.O. Box 918/3, Beijing 100039, China*

^g*University of Jing Gangshan, Jiangxi, China*

Abstract

Some extensions of the Standard Model provide Dark Matter candidate particles with sub-GeV mass. These Light Dark Matter particles have been considered for example in Warm Dark Matter scenarios (e.g. the keV scale sterile neutrino, axino or gravitino). Moreover MeV scale DM candidates have been proposed in supersymmetric models and as source of the 511 keV line from the Galactic center. In this paper the possibility of direct detection of a Light Dark Matter candidate is investigated considering the inelastic scattering processes on the electron or on the nucleus targets. Some theoretical arguments are developed and related phenomenological aspects are discussed. Allowed volumes and regions for the characteristic phenomenological parameters of the considered scenarios are derived from the DAMA/NaI annual modulation data.

Keywords: Light Dark Matter; underground Physics

PACS numbers: 95.35.+d

1 Introduction

Some extensions of the Standard Model provide Dark Matter (DM) candidate particles with sub-GeV mass; in the following these candidates will be indicated as Light Dark Matter (LDM).

Light Dark Matter particles have been considered for example in Warm Dark Matter scenarios such as e.g. keV-scale sterile neutrino [1], axino or gravitino [2]. In

addition, MeV-scale¹ particles (e.g. axino [4], gravitino [5], heavy neutrinos [6, 7], moduli fields from string theories [8], *Elko* fermions [9]) have been proposed as dark matter and as source of 511 keV gamma's from the Galactic center, due either to DM annihilation [10, 11] or to decay² [4, 7] in the bulge. Moreover, also supersymmetric models exist where the LSP naturally has a MeV-scale mass and the other phenomenological properties, required to generate the 511 keV gammas in the galactic bulge [13].

In this paper the direct detection of LDM candidate particles is investigated considering the possible inelastic scattering channels either on the electron or on the nucleus target. We note, in fact, that – since the kinetic energy for LDM particles in the galactic halo does not exceed hundreds eV – the elastic scattering of such LDM particles both on electrons and on nuclei yields energy releases well below the energy thresholds of the detectors used in the field; this prevents the exploitation of the elastic scattering as detection approach for these candidates. Thus, the inelastic process is the only possible exploitable one for the direct detection of LDM.

The following process is, therefore, considered for detection (see Fig.1): the LDM candidate (hereafter named ν_H with mass m_H and 4-momentum k_μ) interacts with the ordinary matter target, T , with mass m_T and 4-momentum p_μ . The target T can be either an atomic nucleus or an atomic electron depending on the nature of the ν_H particle interaction. As result of the interaction a lighter particle is produced (hereafter ν_L with mass $m_L < m_H$ and 4-momentum k'_μ) and the target recoils with an energy E_R , which can be detectable by suitable detectors.

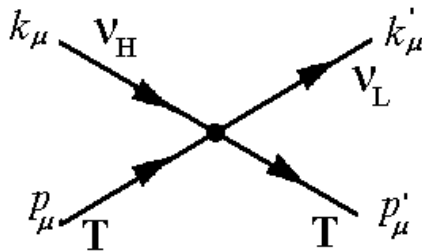


Figure 1: Inelastic scattering process considered for the detection of the Light Dark Matter candidate. The 4-momenta are defined in the laboratory frame. The target T can be either an atomic nucleus or an atomic electron.

The lighter particle ν_L is neutral and it is required that it interacts very weakly with ordinary matter; thus, the ν_L particle escapes the detector. In particular, the ν_L particle can also be another DM halo component (dominant or subdominant with respect to the ν_H one), or it can simply be a Standard Model particle (e.g. ν_L can be identified with an active neutrino in the scenario of the MeV axino of ref. [4], where the diagrams $\tilde{a} + e^- \rightarrow \nu_{\mu,\tau} + e^-$ have been considered).

¹It is worth to note that MeV Dark Matter particles can also be considered for a possible solution of the missing satellite problem [3].

²We also remind that the possible decay of DM particles into a lighter state, with MeV scale splitting, has been considered in refs. [12].

The production mechanism of the ν_H (and eventually of the ν_L) in the early Universe are beyond the scope of the present paper and can be investigated in the future; however, since $m_H > m_L$, it is important to require that the lifetime of the possible decay of the ν_H particle is longer than the age of the Universe. In particular, we note that the detection process of Fig.1 also offers a possible (unavoidable³) decay channel of ν_H into ν_L and $T\bar{T}$ pair if $m_H > m_L + 2m_T$.

Finally, we remind that a LDM particle detection has already been discussed in ref. [14], where the possible light bosonic (keV mass axion-like particles) Dark Matter candidate has been studied, considering the total conversion of its mass into electromagnetic radiation. In the present case, because of the presence of the ν_L particle in the final state, the LDM can be either a boson or a fermion.

In the following, the direct detection of LDM candidate particles is investigated, some theoretical arguments are developed and related phenomenological aspects are discussed. In particular, the impact of these DM candidates will also be discussed in a phenomenological framework on the basis of the 6.3σ C.L. DAMA/NaI model independent evidence for particle Dark Matter in the galactic halo [15, 16]. We remind that various corollary analyses, considering some of the many possible astrophysical, nuclear and particle Physics scenarios, have been analysed by DAMA itself [14, 15, 16, 17, 18, 19, 20], while several others are also available in literature, such as e.g. refs. [21, 22, 23, 24, 25, 26, 27, 28, 29, 30]. Many other scenarios can be considered as well. At present the new second generation DAMA/LIBRA set-up is running at the Gran Sasso National Laboratory of the I.N.F.N..

2 Detectable energy in the inelastic scattering

In this section the recoil energy, E_R , of the target T for the process of Fig.1 is evaluated.

Considering a Lorentz transformation with $\vec{\beta} = \frac{\vec{k} + \vec{p}}{k_0 + p_0}$ (hereafter k_0 , k'_0 , p_0 and p'_0 are the time components of the respective 4-momenta in the laboratory frame, see Fig.1), it is possible to evaluate the energy conservation relation in the center of mass (CM) frame:

$$\sqrt{s} = k_{0,CM} + p_{0,CM} = k'_{0,CM} + p'_{0,CM}. \quad (1)$$

Knowing that $|\vec{k}'_{CM}| = |\vec{p}'_{CM}|$, one obtains:

$$p'_{0,CM} = \frac{m_T^2 - m_L^2}{2\sqrt{s}} + \frac{\sqrt{s}}{2} = \sqrt{p_{CM}^2 + m_T^2}. \quad (2)$$

Defining the Lorentz boost factor: $\gamma = 1/\sqrt{1 - \beta^2} = \frac{k_0 + p_0}{\sqrt{s}}$ one can write the total energy of the target in the laboratory frame after the scattering by means of a Lorentz transformation:

$$p'_0 = \gamma \left(p'_{0,CM} + \vec{\beta} \cdot \vec{p}'_{CM} \right) \quad (3)$$

Assuming the target at rest before the scattering, i.e. $\vec{p} = 0$ and $p_0 = m_T$, and the non-relativistic nature of the LDM particle, i.e. $k_0 \simeq m_H$ and $k \simeq m_H v_{LDM}$, with

³All the other decay channels requires the knowledge/assumptions of some other particle couplings.

$v_{LDM} \sim 10^{-3}c$, the energy released to the target T : $E_R = k_0 - k'_0 = p'_0 - p_0$ (that is, the target recoil energy) can be written as:

$$E_R = p'_0 - m_T = (\gamma p'_{0,CM} - m_T) + \gamma\beta p'_{CM} \cos\theta_{CM} \quad (4)$$

$$= \langle E_R \rangle + \frac{E_+ - E_-}{2} \cos\theta_{CM} \quad (5)$$

where: i) θ_{CM} is the scattering angle in the CM frame; ii) $\langle E_R \rangle$ is the average energy; iii) E_- is the minimum recoil energy; iv) E_+ is the maximum recoil energy.

Considering the non-relativistic nature of the LDM, one gets: $s \simeq (m_T + m_H)^2$, and for the $\langle E_R \rangle$ average energy:

$$\langle E_R \rangle = \frac{E_+ + E_-}{2} \simeq \frac{\bar{m} \Delta}{m_H + m_T}. \quad (6)$$

There $\Delta = m_H - m_L$ is the mass splitting of the $\nu_H - \nu_L$ particle system and $\bar{m} = \frac{m_H + m_L}{2}$ is the average mass of the $\nu_H - \nu_L$ particle system.

The spread of the recoil energy:

$$\frac{E_+ - E_-}{\langle E_R \rangle} \simeq k \sqrt{\frac{8m_T}{\bar{m} \Delta (m_H + m_T)}} \quad (7)$$

can be appreciable only for hundreds MeV LDM interacting on heavy nucleus targets. As an example, assuming $m_H = 1$ MeV and $\Delta = 0.5$ MeV, the spread in energy is few 10^{-3} both for electrons and for every nuclear targets. Therefore, since the LDM kinetic energy is expected to be negligible with respect to Δ , one has: $\langle E_R \rangle \gg (E_+ - E_-)$, and the recoil energy is approximatively fixed at the $\langle E_R \rangle$ value.

In order to offer to the reader just a view of the detectability of LDM particles, Fig. 2 shows examples of the configurations in the plane Δ vs m_H (shaded areas), corresponding to released energies in NaI(Tl) within the energy interval 1-6 keV electron equivalent. The lower area in Fig. 2 refers to LDM interacting on electron targets, while the upper area refers to LDM interacting on the Na and I targets (the effect of the quenching factor [15] and of the channeling in the NaI lattice [19] have been considered). The dashed line $m_H = \Delta$ marks the configurations where ν_L is a massless particle (or also a very light particle, such as e.g. an active neutrino or a nearly massless sterile one or the light axion, etc.). The configurations characterized by $\Delta \geq 2m_e$ (dark area; hereafter m_e is the electron mass) are of interest for the positron annihilation line from the galactic center due to possible (energetically allowed) decay: $\nu_H \rightarrow \nu_L e^+ e^-$. Finally, the configurations on the right of the vertical line at $m_H = 511$ keV are of interest for the possible annihilation process: $\nu_H \bar{\nu}_H \rightarrow e^+ e^-$ in the galactic center, while the configurations of m_H on the right of the solid or dotted curves are of interest for the possible annihilation processes: $\nu_H \bar{\nu}_L \rightarrow e^+ e^-$ (solid curve), $\nu_L \bar{\nu}_H \rightarrow e^+ e^-$ (solid curve), and $\nu_L \bar{\nu}_L \rightarrow e^+ e^-$ (dotted curve) in the galactic center.

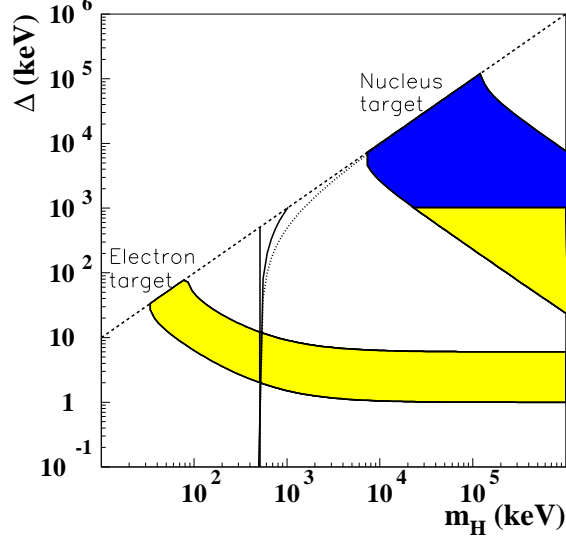


Figure 2: Configurations in the plane Δ vs m_H (shaded areas), corresponding to released energies in NaI(Tl) within the energy interval 1-6 keV electron equivalent. The upper area is due to LDM interaction on Na and I nuclear targets, while the lower area to LDM interaction on electron target. The dashed line ($m_H = \Delta$) marks the case where ν_L is a massless particle. The configurations characterized by $\Delta \geq 2m_e$ (dark area) are of interest for the positron annihilation line from the galactic center through the decay: $\nu_H \rightarrow \nu_L e^+ e^-$. The thresholds of the possible annihilation processes: $\nu_H \bar{\nu}_H \rightarrow e^+ e^-$ (solid vertical line at $m_H = 511$ keV); $\nu_H \bar{\nu}_L \rightarrow e^+ e^-$ (solid curve); $\nu_L \bar{\nu}_H \rightarrow e^+ e^-$ (solid curve); $\nu_L \bar{\nu}_L \rightarrow e^+ e^-$ (dotted curve) are shown.

3 Interaction rate of LDM particle

The interaction rate of the LDM particle with the target T and for the studied process can be written as:

$$\frac{dR_T}{dE_R} = \eta_T \frac{\rho_{\nu_H}}{m_H} \int \frac{d\sigma_T}{dE_R} v f(\vec{v}) d^3v, \quad (8)$$

where: i) $\rho_{\nu_H} = \xi \rho_0$, with ρ_0 local halo density and $\xi \leq 1$ fractional amount of ν_H density in the halo; ii) η_T is the target number density in the detector; iii) $\frac{d\sigma_T}{dE_R}$ is the differential cross section of the considered LDM particle inelastic scattering with the target T ; iv) $f(\vec{v})$ is the velocity (\vec{v}) distribution of the ν_H particles in the Earth (laboratory) frame.

Since the sub-GeV LDM wavelength ($\lambda = \frac{h}{k} > 10^3$ fm) is much larger than the nucleus size, the targets can be considered as point-like and the form factors of the targets can be approximated by unity. In such a reasonable hypothesis and assuming,

for simplicity, the isotropy of the differential cross section⁴, one gets:

$$\frac{d\sigma_T}{dE_R} \simeq \frac{\sigma_T}{E_+ - E_-} \Theta(E_+ - E_R) \Theta(E_R - E_-), \quad (9)$$

where: i) σ_T is the target cross section; ii) the Heaviside functions, Θ , define the domain of the differential cross section. We note that E_+ and E_- depend on the target mass and slightly on the LDM velocity, v .

Generally, σ_T can be a function of v , depending on the peculiarity of the particle interaction. In the following, we adopt a widely considered approximation for the non-relativistic case [11, 13, 31] (the subscript T drops):

$$\sigma v \simeq a + bv^2. \quad (10)$$

There a and b are constant and depend on the peculiarity of the particle interaction with the target T ; they will be considered as free parameters in the description of the process. In the following, in order to deal the direct detection process with more usual parameters, the cross sections $\sigma_0^T = \frac{a}{v_0}$ and $\sigma_m^T = bv_0$ will be used as free parameters; they are related to the a and b parameters rescaled with the Dark Matter local velocity, v_0 , [32, 33].

Thus, eq. (8), becomes:

$$\frac{dR_T}{dE_R} = \eta_T \frac{\rho_{\nu H}}{v_0 m_H} \int (\sigma_0^T v_0^2 + \sigma_m^T v^2) \frac{\Theta(E_+ - E_R) \Theta(E_R - E_-)}{E_+ - E_-} f(\vec{v}) d^3 v. \quad (11)$$

Since: $\int_0^\infty \frac{\Theta(E_+ - E_R) \Theta(E_R - E_-)}{E_+ - E_-} dE_R = 1$, the total rate R_T^{tot} can be written as:

$$R_T^{tot} = \int_0^\infty \frac{dR_T}{dE_R} dE_R = \eta_T \frac{\rho_{\nu H}}{v_0 m_H} (\sigma_0^T v_0^2 + \sigma_m^T \langle v^2 \rangle). \quad (12)$$

Similarly as the light bosonic case discussed in ref. [14], the $\sigma_m^T \langle v^2 \rangle$ term provides an annual modulation of the expected counting rate for LDM interactions. In fact, the velocity of the LDM particle in the galactic frame can be defined as: $\vec{v}_g = \vec{v} + \vec{v}_\oplus$. Thus, one obtains for non rotating halo: $\langle v^2 \rangle = \langle v_g^2 \rangle + v_\oplus^2$. Since the Earth velocity in the galactic frame (\vec{v}_\oplus) is given by the sum of the Sun velocity (\vec{v}_\odot) and of the Earth's orbital time-dependent velocity around the Sun ($\vec{v}_{SE}(t)$), neglecting the v_{SE}^2 term one gets:

$$\langle v^2 \rangle \simeq \langle v_g^2 \rangle + v_\odot^2 + 2\vec{v}_\odot \cdot \vec{v}_{SE}(t) \simeq \langle v_g^2 \rangle + v_\odot^2 + v_\odot v_{SE} \cos(\omega(t - t_0)). \quad (13)$$

In the last equation the angle of the terrestrial orbit with respect to the galactic plane has been considered to be $\simeq 60^\circ$. Moreover, we consider $\omega = 2\pi/T$ with $T = 1$ year, and the phase t_0 (which corresponds to $\simeq 2$ nd June, that is, when the Earth's speed in the galactic frame is at the maximum). The Sun velocity can be written as $|\vec{v}_\odot| \simeq v_0 + 12$ km/s, where v_0 is the local velocity, whose value is in the range 170-270 km/s [32, 33]. The Earth's orbital velocity is $v_{SE} \simeq 30$ km/s. Finally, $\langle v_g^2 \rangle$ depends on the halo model and on the v_0 value (just for reference, in the particular simplified case of isothermal halo model: $\langle v_g^2 \rangle = \frac{3}{2}v_0^2$).

⁴Different assumptions would produce quite similar phenomenologies, since – as mentioned – $\langle E_R \rangle \gg (E_+ - E_-)$, and the recoil energy is approximatively fixed at the $\langle E_R \rangle$ value.

In conclusion, the expected signal is given by the sum of two contributions: one independent on the time and the other one dependent on the time through $\cos(\omega(t - t_0))$, with relative amplitude depending on the adopted scenario.

3.1 Interaction with atomic electrons

For atomic electron targets, the energy interval (E_-, E_+) is always very narrow $\left(\frac{E_+ - E_-}{\langle E_R \rangle} \lesssim few\ \%\right)$. Therefore, using the approximation $\frac{\Theta(E_+ - E_R)\Theta(E_R - E_-)}{E_+ - E_-} \simeq \delta(E_R - \langle E_R \rangle)$, the interaction rate with atomic electrons can be simply written as:

$$\frac{dR_e}{dE_R} \simeq \eta_e \frac{\rho_{\nu H}}{v_0 m_H} (\sigma_0^e v_0^2 + \sigma_m^e \langle v^2 \rangle) \delta(E_R - \langle E_R \rangle) \quad (14)$$

where η_e is the electron number density in the target detector and σ_0^e and σ_m^e are the average (over all the atomic electrons) cross section parameters for electrons in the target material.

After the interaction the final state can have – beyond the ν_L particle – either a prompt electron and an ionized atom or an excited atom plus possible X-rays/Auger electrons. Therefore, the process produces X-rays and electrons of relatively low energy, which are mostly contained with efficiency $\simeq 1$ in a detector of a suitable size.

Therefore, the differential counting rate can simply be written accounting for the detector energy resolution, by means of the $G(E, E_R)$ kernel, which generally has a Gaussian behaviour:

$$\frac{dR_e}{dE} = \int G(E, E_R) \frac{dR_e}{dE_R} dE_R = R_e^{tot} \times \frac{1}{\sqrt{2\pi}\delta} e^{-\frac{(E - \langle E_R \rangle)^2}{2\delta^2}}. \quad (15)$$

There δ is the energy resolution of the detector and R_e^{tot} is the area of the Gaussian peak centered at the $\langle E_R \rangle$ value.

Finally, the expected differential rate is given by the sum of two contributions: $\frac{dR_e}{dE} = S_0 + S_m \cdot \cos\omega(t - t_0)$, where S_0 and S_m are the unmodulated and the modulated part of the expected differential counting rate, respectively.

3.2 Interaction with nuclei

As regards the interaction with target nuclei, when considering the cases of heavy target and for relatively “high” LDM mass the energy interval (E_-, E_+) cannot be neglected. Therefore, the interaction rate with the nucleus T can be approximated as:

$$\frac{dR_T}{dE_R} \simeq \eta_T \frac{\rho_{\nu H}}{v_0 m_H} (\sigma_0^T v_0^2 + \sigma_m^T \langle v^2 \rangle) \frac{\Theta(E_+^T - E_R)\Theta(E_R - E_-^T)}{E_+^T - E_-^T}, \quad (16)$$

where η_T is the nucleus number density in the material and E_{\pm}^T are the E_{\pm} values for the nucleus T calculated at $v = \langle v \rangle$.

Considering the case of a crystal detector target (as e.g. the NaI(Tl)), the possible channeling effect [19] has also to be taken into account. The detection of a nuclear recoil of kinetic energy, E_R , is, in particular, related to the response function $\frac{dN_T}{dE_{det}}(E_{det}|E_R)$

[19], where E_{det} is the released energy in keV electron equivalent. Thus, the differential E_{det} distribution for the nucleus T when accounting for the channeling effect can be written as:

$$\frac{dR_T^{(ch)}}{dE_{det}}(E_{det}) = \int \frac{dN_T}{dE_{det}}(E_{det}|E_R) \frac{dR_T}{dE_R}(E_R) dE_R . \quad (17)$$

Hence, the expected differential counting rate for LDM interaction with nucleus T can easily be derived accounting for the detector energy resolution kernel $G(E, E_{det})$:

$$\frac{dR_T^{(ch)}}{dE} = \int G(E, E_{det}) \frac{dR_T^{(ch)}}{dE_{det}} dE_{det} . \quad (18)$$

Finally, as for the electron interacting LDM, the expected differential rate is given by the sum of two contributions: $\frac{dR_T}{dE} = S_0 + S_m \cdot \cos\omega(t - t_0)$, where S_0 and S_m are the unmodulated and the modulated part of the expected differential counting rate, respectively.

3.3 Some examples on interaction rate in NaI(Tl)

In this section as template purpose, some examples on interaction rate of LDM particles in NaI(Tl) detectors are given. In particular, since the expected energy distribution for electron⁵ interacting LDM has a simple Gaussian behaviour (see eq. (15)), only some examples for the nucleus interacting LDM will be shown in the following.

In NaI(Tl) detectors, both Na and I nuclei ($\eta_{Na} = \eta_I \simeq 4 \times 10^{24} \text{ kg}^{-1}$) can contribute to the detection of LDM. Therefore, the total expected counting rate is given by the sum of two contributions similar as eq. (18), arising from the two nuclei species ($T = \text{Na}, \text{I}$). The cross section parameters σ_0^T and σ_m^T for Na and I are related with some model dependent scaling laws; in particular, in the following, the two illustrative cases of coherent ($\sigma^{coh} \simeq \frac{\sigma^{Na}}{A_{Na}^2} \simeq \frac{\sigma^I}{A_I^2}$) and incoherent ($\sigma^{inc} \simeq \sigma^{Na} \simeq \sigma^I$) nuclear scaling laws are investigated. Obviously, other different nuclear scaling laws are in principle possible.

As template purpose, in Fig. 3, the expected energy distributions of the unmodulated/modulated part of the differential rate in NaI(Tl) are shown for interactions of LDM with $m_H = 100 \text{ MeV}$ on the target nuclei. In particular, there are shown the cases of coherent cross section scaling laws (Fig. 3 *-left*) with $\Delta = 4.8 \text{ MeV}$ and $\xi\sigma_0^{coh} \ll \xi\sigma_m^{coh} \simeq 2 \times 10^{-6} \text{ pb}$ and the case of incoherent cross section scaling laws (Fig. 3 *-right*) with $\Delta = 0.95 \text{ MeV}$ and $\xi\sigma_0^{inc} \ll \xi\sigma_m^{inc} \simeq 20 \times 10^{-3} \text{ pb}$. The A5 halo model (a NFW halo model with local velocity equal to 220 km/s and density equal to the maximum value, see ref. [15, 16]) has been considered. The quenching factors have been assumed as the case A of ref. [15, 16] and the channeling effect has been included, as mentioned.

It is worthwhile to note that similar behaviors can also be obtained by using other choices of the halo model, quenching factors and values of the masses of the involved particles in the interaction.

⁵Here, we only remind that $\eta_e \simeq 2.6 \times 10^{26} \text{ kg}^{-1}$ in NaI(Tl).

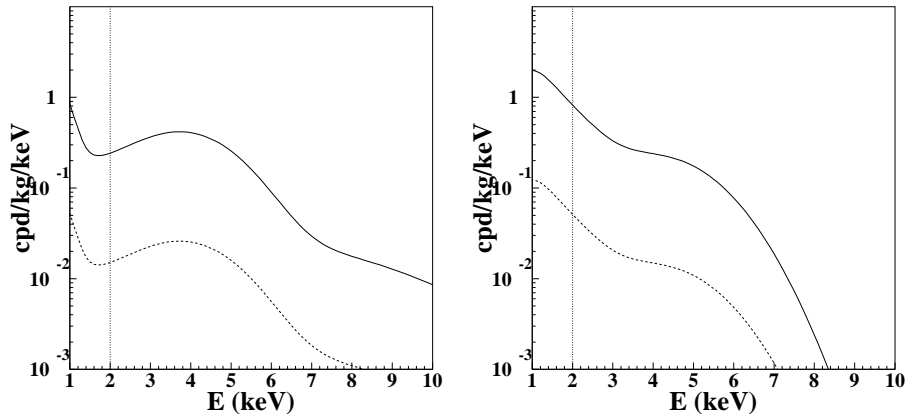


Figure 3: Examples of the energy distributions of the unmodulated (solid) and of the modulated (dotted) parts of the expected differential rate in NaI(Tl) for interactions of LDM with $m_H = 100$ MeV on the target nuclei. *Left*: case of coherent cross section scaling laws; here $\Delta = 4.8$ MeV and $\xi\sigma_0^{coh} \ll \xi\sigma_m^{coh} \simeq 2 \times 10^{-6}$ pb. *Right*: case of incoherent cross section scaling laws; here $\Delta = 0.95$ MeV and $\xi\sigma_0^{inc} \ll \xi\sigma_m^{inc} \simeq 20 \times 10^{-3}$ pb. The A5 halo model (a NFW halo model with local velocity equal to 220 km/s and density equal to the maximum value, see ref. [15, 16]) has been considered. The quenching factors have been assumed as the case A of ref. [15, 16]. The channeling effect has been included; see text. The vertical dotted lines correspond to the energy threshold of the NaI(Tl) detectors used in DAMA/NaI set-up.

4 Data analysis and results for LDM candidates in DAMA/NaI

The 6.3σ C.L. model independent evidence for Dark Matter particles in the galactic halo achieved over seven annual cycles by DAMA/NaI [15, 16] (total exposure $\simeq 1.1 \times 10^5$ kg \times days) can also be investigated for the case of a LDM candidate (in addition to the other corollary quests analyzed by DAMA itself [14, 15, 16, 17, 18, 19, 20] and available in literature, e.g. refs. [21, 22, 23, 24, 25, 26, 27, 28, 29, 30]).

In the following, the same dark halo models and related parameters given in table VI of ref. [15] are considered. The related DM density is given in table VII of the same reference. Note that, although a large number of self-consistent galactic halo models have been considered, still many other possibilities exist. As regards the case of LDM interacting on nuclei, also the Na and I quenching factors [15] and the Na and I channeling response functions given in [19] have been considered. The uncertainties on the Na and I quenching factors have been taken into account as done in ref. [15]. In addition, the presence of the existing Migdal effect and of the possible SagDEG contributions – we discussed in [18, 17], respectively – will be not included here for simplicity.

As regards the cross section parameters, the σ_0 terms do not contribute to the

annual modulation of the signal. In particular, the measured modulation amplitude easily allows to derive $\sigma_0 \lesssim \sigma_m$. In the following, for simplicity, the contributions of the σ_m terms are assumed to be dominant with respect to the contributions of the σ_0 ones.

The results are calculated by taking into account the time and energy behaviours of the *single-hit*⁶ experimental data through the standard maximum likelihood method⁷. In particular, they are presented in terms of slices of the three-dimensional allowed volume $(m_H, \Delta, \xi\sigma_m)$ – where σ_m is alternatively σ_m^e , σ_m^{coh} and σ_m^{inc} – obtained as superposition of the configurations corresponding to likelihood function values *distant* more than 4σ from the null hypothesis (absence of modulation) in each one of the several (but still a very limited number) of the considered model frameworks. In this way one accounts for at least some of the existing theoretical and experimental uncertainties. It is worth to note that the inclusion of other existing uncertainties would further extend the allowed volumes/regions and increase the sets of obtained best fit values.

The projection of the whole 4σ allowed volume on the plane (m_H, Δ) gives typical patterns similar as those reported in Fig.2. Moreover, since the two regions are disconnected, the LDM detection is always dominated by only one of the different target contributions. Therefore, in the following, slices of the allowed volume either for electron interacting LDM or nucleus interacting LDM are presented separately.

4.1 Case of electron interacting LDM

In case of electron interacting LDM, the projection of the 4σ allowed volume on the plane (m_H, Δ) for the same dark halo models and parameters described in ref. [15] is reported in Fig.4. The allowed m_H values and the splitting Δ are in the intervals $35 \text{ keV} \lesssim m_H \lesssim \text{O}(\text{GeV})$ ⁸ and $1 \text{ keV} \lesssim \Delta \lesssim 80 \text{ keV}$, respectively. It is worth to note that in such a case the decay through the detection channel: $\nu_H \rightarrow \nu_L e^+ e^-$, is energetically forbidden for the given Δ range. The configurations with $m_H \gtrsim 511 \text{ keV}$ (dark area in Fig.4) are instead of interest for the possible annihilation processes: $\nu_H \bar{\nu}_H \rightarrow e^+ e^-$, $\nu_H \bar{\nu}_L \rightarrow e^+ e^-$, $\nu_L \bar{\nu}_H \rightarrow e^+ e^-$, and $\nu_L \bar{\nu}_L \rightarrow e^+ e^-$, in the galactic center.

As examples, some slices of the 3-dimensional allowed volume for various m_H values in the $(\xi\sigma_m^e \text{ vs } \Delta)$ plane are depicted in Fig.5–*left* in the scenario given above.

⁶The *single-hit* events are those events where only one detector of many actually fires in a multi-detectors set-up. In particular, the ν_H particle is no more present after the inelastic interaction and, therefore, can only provide *single-hit* events in a multi-detectors set-up.

⁷Shortly, the likelihood function is: $\mathbf{L} = \prod_{ijk} e^{-\mu_{ijk}} \frac{\mu_{ijk}^{N_{ijk}}}{N_{ijk}!}$, where N_{ijk} is the number of events collected in the i -th time interval, by the j -th detector and in the k -th energy bin. N_{ijk} follows a Poissonian distribution with expectation value $\mu_{ijk} = [b_{jk} + S_{0,k} + S_{m,k} \cdot \cos\omega(t_i - t_0)] M_j \Delta t_i \Delta E \epsilon_{jk}$. The unmodulated and modulated parts of the signal, $S_{0,k}$ and $S_{m,k} \cos\omega(t_i - t_0)$, respectively, are here functions of the LDM mass m_H , the splitting Δ and the cross section σ_m . The b_{jk} is the background contribution; Δt_i is the detector running time during the i -th time interval; ΔE is the energy bin; ϵ_{jk} is the overall efficiency and M_j is the detector mass.

⁸ For values of m_H greater than $\text{O}(\text{GeV})$, the definition of Light Dark Matter is no more appropriate. Moreover, the kinetic energy of the particle would be enough for the detection also through the elastic scattering process, as demonstrated in ref. [20].

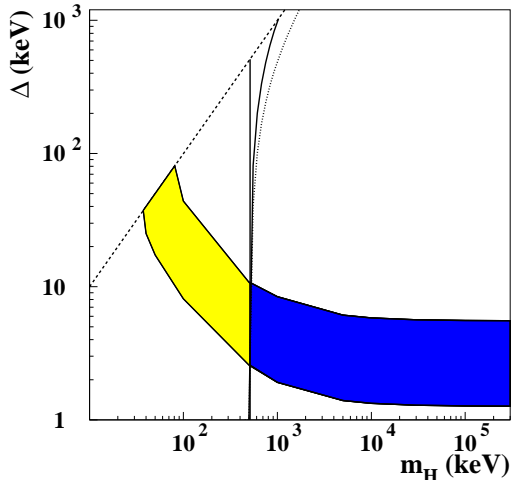


Figure 4: Case of electron interacting LDM. Projection of the 4σ allowed 3-dimensional volume on the plane (m_H, Δ) for the same dark halo models and parameters described in ref. [15]; see text. The dashed line ($m_H = \Delta$) marks the case where ν_L is a massless particle. The decay through the detection channel, $\nu_H \rightarrow \nu_L e^+ e^-$, is energetically not allowed for the selected configurations. The configurations with $m_H \gtrsim m_e$ (dark area) are interesting for the possible annihilation processes: $\nu_H \bar{\nu}_H \rightarrow e^+ e^-$, $\nu_H \bar{\nu}_L \rightarrow e^+ e^-$, $\nu_L \bar{\nu}_H \rightarrow e^+ e^-$, and $\nu_L \bar{\nu}_L \rightarrow e^+ e^-$ in the galactic center. The three nearly vertical curves are the thresholds of these latter processes as mentioned in the caption of Fig.2 and in the text.

The slice of the 4σ allowed 3-dimensional volume for $m_H = \Delta$ is shown in Fig.5–*right*. This slice has been taken along the dotted line of Fig.4, restricting $m_L \simeq 0$, that is for a massless or a very light ν_L particle, such as e.g. either an active neutrino or a nearly massless sterile one or the light axion, etc.

Finally, it is worth to summarize that electron interacting LDM candidates in the few-tens-keV/sub-MeV range are allowed (see Figs.4 and 5). This can be of interest for example in the models of Warm Dark Matter particles – such as e.g. Weakly Sterile Neutrino [1], Axino or Gravitino [2] – or in the models where the DM is made of Moduli fields [8]. Moreover, also configurations with m_H in the MeV/sub-GeV range are allowed; similar LDM candidates (such as e.g. axino [4], sterile neutrino [7], moduli fields from string theories [8], and even MeV-scale LSP in supersymmetric theories [13]) can also be of interest for the production mechanism of the 511 keV gammas from the galactic bulge [10, 11].

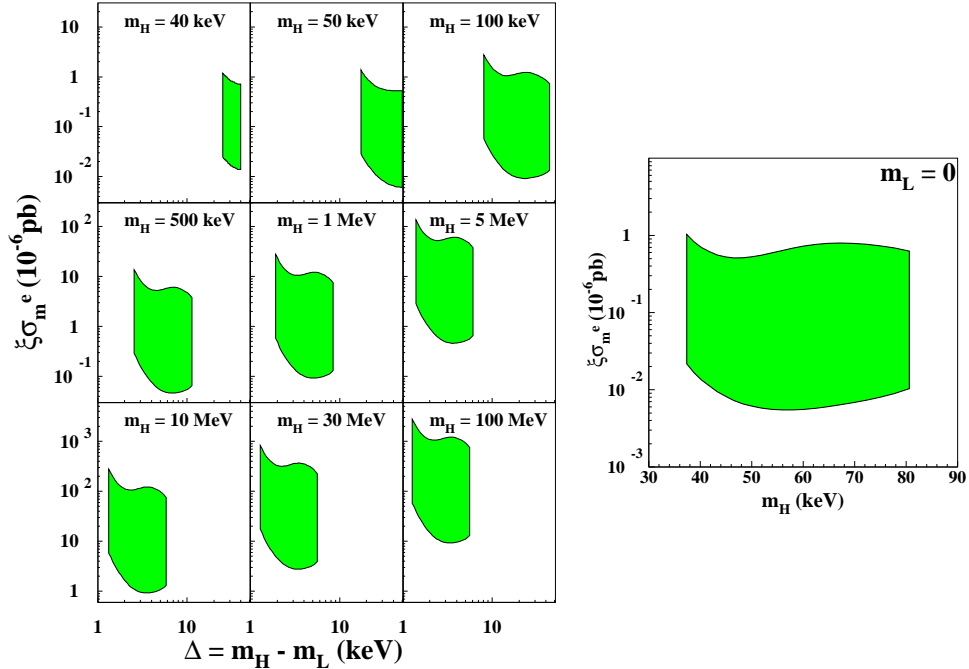


Figure 5: Case of electron interacting LDM. *Left*: examples of some slices of the 4σ allowed 3-dimensional volume for various m_H depicted in the $(\xi\sigma_m^e$ vs Δ) plane. *Right*: slice of the 4σ allowed 3-dimensional volume for $m_H = \Delta$, that is for a massless or a very light ν_L particle, as e.g. either an active neutrino or a nearly massless sterile one or the light axion, etc. The same dark halo models and parameters described in ref. [15] have been used; see text.

4.2 Case of nucleus interacting LDM

In case of nucleus interacting LDM, the projections of the 4σ allowed volumes on the plane (m_H, Δ) are reported in Fig.6 for the two above-mentioned illustrative cases of coherent (*left*) and incoherent (*right*) nuclear scaling laws. They are evaluated for the same dark halo models and parameters described in ref. [15, 19]. The allowed m_H values and the splitting Δ are in the intervals $8 \text{ MeV} \lesssim m_H \lesssim \text{O}(\text{GeV})^9$ and $25 \text{ keV} \lesssim \Delta \lesssim 120 \text{ MeV}$, respectively (see Fig.6). It is worth to note that in such a case the decays through the diagram involved in the detection channel (e.g. in nucleon anti-nucleon pairs or in meson(s), as $\nu_H \rightarrow \nu_L \pi^0$) are obviously energetically forbidden. Moreover, there are allowed configurations that could contribute – in principle, if suitable couplings exist – to the positron generation in the galactic center; in fact, the decay $\nu_H \rightarrow \nu_L e^+ e^-$ is energetically allowed for $\Delta > 2m_e$ (dark area in Fig.6), while the annihilation processes into $e^+ e^-$ pairs are energetically allowed for almost all the

⁹We remind that for m_H values greater than $\text{O}(\text{GeV})$ the detection would also be possible through the elastic scattering process [15, 16, 17, 18, 19].

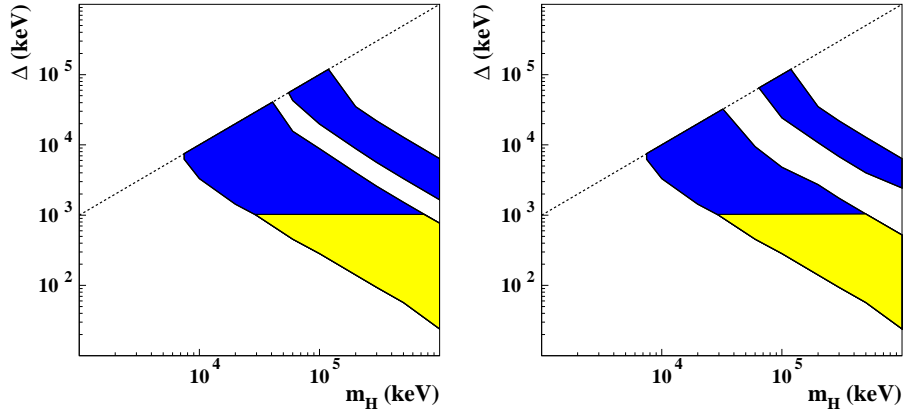


Figure 6: Case of nucleus interacting LDM. Projections of the 4σ allowed 3-dimensional volumes on the plane (m_H, Δ) for the two above-mentioned illustrative cases of coherent (*left*) and incoherent (*right*) nuclear scaling laws. They are evaluated for the same dark halo models and parameters described in ref. [15, 19]. The regions enclose configurations corresponding to likelihood function values *distant* more than 4σ from the null hypothesis (absence of modulation). The dashed lines ($m_H = \Delta$) mark the case where ν_L is a massless particle. The decays through the diagram involved in the detection channel are energetically forbidden. See text.

allowed configurations.

It is worth to note that for nuclear interacting LDM the 3-dimensional allowed configurations are contained in two disconnected volumes, as seen e.g. in their projections in Fig. 6. The one at larger Δ at m_H fixed is mostly due to interaction on Iodine target, while the other one is mostly due to interaction on Sodium target.

As examples, some slices of the 3-dimensional allowed volumes for various m_H values in the $(\xi\sigma_m$ vs $\Delta)$ plane are depicted in Fig.7 for the two above-mentioned illustrative cases of coherent (*left* panel) and incoherent (*right* panel) nuclear scaling laws.

The slices of the 4σ allowed 3-dimensional volumes for $m_H = \Delta$ are shown in Fig.8 for the two illustrative cases of coherent (*left* panel) and incoherent (*right* panel) nuclear scaling laws. These slices have been taken along the dotted lines of Fig.6, restricting $m_L \simeq 0$, that is for a massless or a very light ν_L particle, as e.g. either an active neutrino or a nearly massless sterile one or the light axion, etc.

Finally, it is worth to summarize that LDM candidates in the MeV/sub-GeV range are allowed (see Figs.6, 7 and 8). Also these candidates, such as e.g. axino [4], sterile neutrino [7], moduli fields from string theories [8], and even MeV-scale LSP in supersymmetric theories [13], can be of interest for the positron production in the galactic center [10, 11].

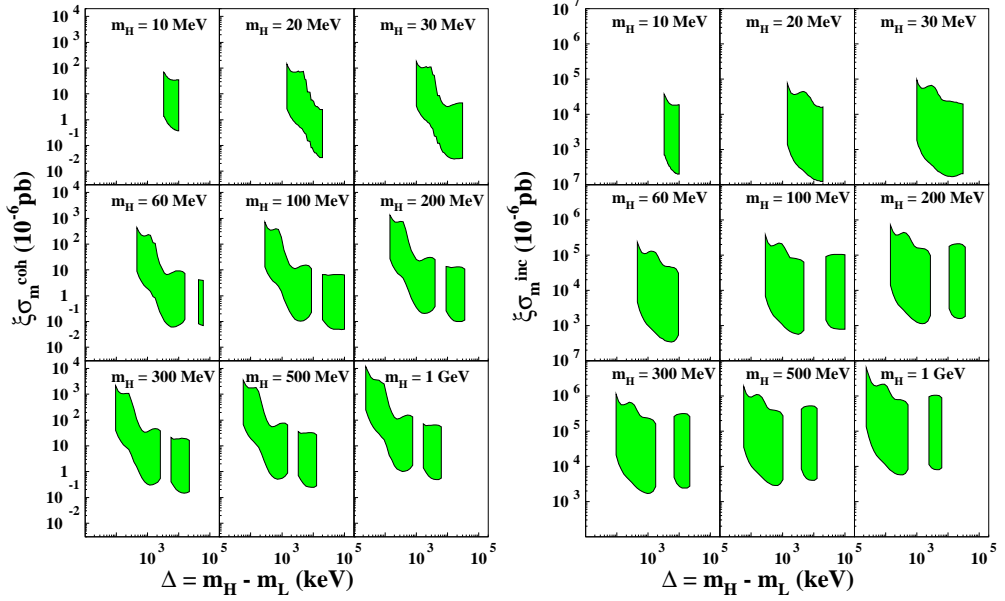


Figure 7: Case of nucleus interacting LDM. Examples of some slices of the 3-dimensional allowed volumes for various m_H values in the $(\xi\sigma_m$ vs Δ) plane for the two above-mentioned illustrative cases of coherent (*left*) and incoherent (*right*) nuclear scaling laws. The 3-dimensional volumes enclose configurations corresponding to likelihood function values *distant* more than 4σ from the null hypothesis (absence of modulation). The same dark halo models and parameters described in ref. [15, 19] have been used.

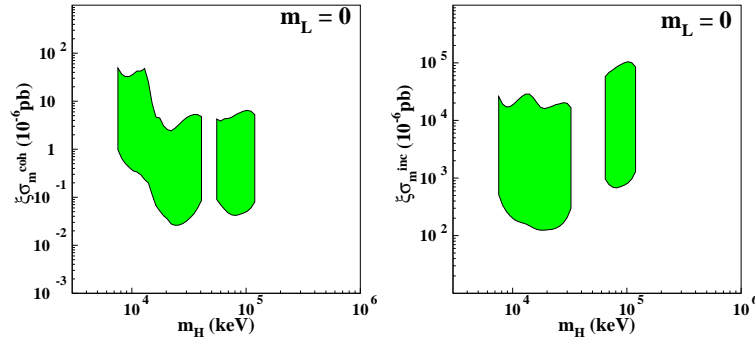


Figure 8: Case of nucleus interacting LDM. Slices of the 4σ allowed 3-dimensional volumes for $m_H = \Delta$, that is for a massless or a very light ν_L particle, as e.g. either an active neutrino or a nearly massless sterile one or the light axion, etc. They are evaluated for the two illustrative cases of coherent (*left* panel) and incoherent (*right* panel) nuclear scaling laws, using the same dark halo models and parameters described in ref. [15, 19].

5 Conclusions

In this paper, the possibility of direct detection of a Light Dark Matter candidate particle has been investigated. The inelastic scattering processes on the electron or on the nucleus targets have been considered; these are the only possible processes useful for the direct detection of such LDM candidates.

Some theoretical arguments have been developed and related phenomenological aspects have been discussed. In particular, the impact of the LDM candidate has also been analyzed in a phenomenological framework on the basis of DAMA/NaI annual modulation data. Allowed volumes and regions for the characteristic phenomenological parameters have been derived in the considered model. The allowed phenomenological parameters (masses and cross sections) of LDM can be of interest for various LDM candidates proposed in theories beyond the Standard Model and for the production mechanism of the 511 keV gammas from the galactic bulge.

In conclusion this paper has shown that – in addition to other candidates, as WIMP/WIMP-like particles and axion-like bosons, already discussed by DAMA collaboration elsewhere [14, 15, 16, 17, 18, 19, 20] – there is also possibility for a LDM candidate interacting either with the electrons or with the nuclei to account for the 6.3σ C.L. model independent evidence for the presence of a particle DM component in the galactic halo.

References

- [1] see e.g.: A. Kusenko, AIP Conf. Proc. 917 (2007) 58;
A. Palazzo et al., Phys. Rev. D 76 (2007) 103511;
M. Shaposhnikov, Nucl. Phys. B 763 (2007) 49;
R. Volkas, Prog. Part. Nucl. Phys. 48 (2002) 161.
- [2] see e.g.: F. D. Steffen arXiv:0711.1240[hep-ph];
A. Brandenburg and F. D. Steffen JCAP 0408 (2004) 008;
O. Seto Phys. Rev. D 75 (2007) 123506;
E. A. Baltz and H. Murayama JHEP 0305 (2003) 067.
- [3] D. Hooper et al. arXiv:0704.2558[astro-ph].
- [4] D. Hooper and L. T. Wang, Phys. Rev. D 70 (2004) 063506.
- [5] M. Lemoine et al., Phys. Lett. B 645 (2007) 222.
- [6] J. M. Frère et al., arXiv:hep-ph/0610240.
- [7] C. Picciotto and M. Pospelov, Phys. Lett. B 605 (2005) 15.
- [8] M. Kawasaki and T. Yanagida Phys. Lett. B 624 (2005) 162;
T. Asaka et al., Phys. Rev. D 58 (1998) 083509;
T. Asaka et al., Phys. Rev. D 58 (1998) 023507.
- [9] D. V. Ahluwalia-Khalilova and D. Grumiller Phys. Rev. D 72 (2005) 067701;
D. V. Ahluwalia-Khalilova and D. Grumiller JCAP 07 (2005) 012.
- [10] C. Boehm et al., Phys. Rev. Lett. 92 (2004) 101301;
P. Fayet, Phys. Rev. D 75 (2007) 115017.

- [11] C. Boehm and Y. Ascasibar, *Phys. Rev. D* 70 (2004) 115013;
Y. Ascasibar et al., *Mon. Not. R. Astron. Soc.* 368 (2006) 1695;
C. Jacoby and S. Nussinov *JHEP* 05 (2007) 17;
P. Fayet *Phys. Rev. D* 70 (2004) 023514.
- [12] D. P. Finkbeiner and N. Wiener, *Phys. Rev. D* 76 (2007) 083519;
J. A. R. Cembranos and L. E. Strigari, arXiv:0801.0630[astro-ph].
- [13] D. Hooper and K.M. Zurek arXiv:0801.3686 [hep-ph].
- [14] R. Bernabei et al., *Int. J. Mod. Phys. A* 21 (2006) 1445.
- [15] R. Bernabei et al., *La Rivista del Nuovo Cimento* 26 n.1 (2003) 1-73.
- [16] R. Bernabei et al., *Int. J. Mod. Phys. D* 13 (2004) 2127.
- [17] R. Bernabei et al., *Eur. Phys. J. C* 47 (2006) 263.
- [18] R. Bernabei et al., *Int. J. Mod. Phys. A* 22 (2007) 3155-3168.
- [19] R. Bernabei et al., *Eur. Phys. J. C* 53 (2008) 205.
- [20] R. Bernabei et al., *Phys. Rev. D* 77 (2008) 023506.
- [21] A. Bottino et al., *Phys. Rev. D* 67 (2003) 063519;
A. Bottino et al., *Phys. Rev. D* 68 (2003) 043506.
- [22] A. Bottino et al., *Phys. Rev. D* 69 (2004) 037302.
- [23] A. Bottino et al., *Phys. Lett. B* 402 (1997) 113;
Phys. Lett. B 423 (1998) 109;
Phys. Rev. D 59 (1999) 095004;
Phys. Rev. D 59 (1999) 095003;
Astrop. Phys. 10 (1999) 203;
Astrop. Phys. 13 (2000) 215;
Phys. Rev. D 62 (2000) 056006;
Phys. Rev. D 63 (2001) 125003;
Nucl. Phys. B 608 (2001) 461.
- [24] K. Belotsky, D. Fargion, M. Khlopov and R.V. Konoplich, hep-ph/0411093.
- [25] D. Smith and N. Weiner, *Phys. Rev. D* 64 (2001) 043502;
D. Tucker-Smith and N. Weiner, *Phys. Rev. D* 72 (2005) 063509.
- [26] R. Foot *Phys. Rev. D* 69 (2004) 036001.
- [27] S. Mitra, *Phys. Rev. D* 71 (2005) 121302(R).
- [28] E.M. Drobyshevski et al., *Astron. & Astroph. Trans.* 26:4 (2007) 289;
E.M. Drobyshevski, arXiv:0706.3095.
- [29] C. Arina and N. Fornengo, arXiv:0709.4477.
- [30] A. Bottino et al., arXiv:0710.0553.
- [31] G. Jungman et al., *Phys. Rep.* 267 (1996) 195;
M.A. Amin and T. Wizansky arXiv:0710.5517.
- [32] P. Belli et al., *Phys. Rev. D* 61 (2000) 023512.
- [33] P.J.T. Leonard and S. Tremaine, *Astrophys. J.* 353 (1990) 486;
C.S. Kochanek, *Astrophys. J.* 457 (1996) 228;
K.M. Cudworth, *Astron. J.* 99 (1990) 590.